Radiation Physics and Chemistry 177 (2020) 109132

Contents lists available at ScienceDirect

Radiation Physics and Chemistry

journal homepage: www.elsevier.com/locate/radphyschem

Thermoluminescence studies of polycrystalline $CaSiO_3$ pellets for photons and particle therapy beams

Carlos D. Gonzales-Lorenzo[a,e,*], Luana F. Nascimento[b], Satoshi Kodaira[c], Monise B. Gomes[d], Shigueo Watanabe[a]

[a] Institute of Physics, University of São Paulo, Rua do Matão, Travessa R, 187, CEP 05508-090, São Paulo, SP, Brazil
[b] SCK·CEN Belgian Nuclear Research Centre, Boeretang 200, Mol, Belgium
[c] Radiation Measurement Research Section, National Institute of Radiological Sciences, Chiba, Japan
[d] Nuclear and Energy Research Institute, IPEN-CNEN/SP, Av. Prof. Lineu Prestes, 2242, Cidade Universitária, 05508-000, São Paulo, SP, Brazil
[e] Escuela Profesional de Física, Facultad de Ciencias Naturales y Formales, Universidad Nacional de San Agustín (UNSA), Av. Independencia S/N, Arequipa, Peru

ARTICLE INFO

Keywords:
$CaSiO_3$ detector
Thermoluminescence
Protons
Carbon
Dosimetry

ABSTRACT

In this work, pellets of $CaSiO_3$ have been produced for investigation as gamma radiation, proton, and carbon ions detector. They were then irradiated to gamma radiation using ^{137}Cs and ^{60}Co sources. Furthermore, pellets of $CaSiO_3$ were exposed to 160 MeV proton and 290 MeV/n carbon ion beam from an upper synchrotron. Thermoluminescence (TL) responses of these pellets presented the same prominent peak at about 170 °C, and two possible high-temperature peaks at 270 and 320 °C when irradiated to gamma, proton, and carbon ion beam. Dose-response curve, minimum detectable dose (MDD), energy dependence, and dependence on the dose rate when irradiated with gamma radiation were evaluated in this material. Linear dose-response curves for proton and carbon ion irradiation have been compared to that of the gamma dose-response. In this way, the dose read out in Harshaw TL reader presented a good agreement with doses found using ion chamber in the case of proton beams and slightly less in the case of carbon beam due to the LET dependency. Furthermore, relative efficiencies of $CaSiO_3$ for beam irradiation of proton and carbon ion display no dependence in the analyzed particle doses range.

1. Introduction

Radiation therapy technologies have advanced rapidly, providing increasingly sophisticated methods to deliver the dose of radiation to the tumor (Jaffray et al., 2010; Spitz et al., 2019; Fujisawa et al., 2013; Mein et al., 2017; Tsujii et al., 2007). Ion beam radiotherapy, such as proton and heavier ions beam has been the subject of considerable debate since the middle of the last century. Nonetheless, it is since the early 1990s that particle therapy began to be used officially in cancer diagnosis and therapy (Tsujii et al., 2007; Mohamad et al., 2018; Takada, 2010; Tsujii, 2014; Barth et al., 2003; Haberer, 2002). In a radiotherapy procedure, when ion beam is involved a dose prescription is required, and an absorbed dose is still required as an operative quantity to control beam delivery with the purpose to characterize the beam dosimetrically and to verify dose delivery (Wambersie et al., 2011; Karger et al., 2010). For that reason, luminescence materials as a good alternative of passive detectors for radiation dose measurement have been studied for decades (Kry et al., 2020; Nascimento et al., 2015; Nakajima et al., 1978; Akselrod et al., 1990; Lakshmanan, 2001; Obryk et al., 2011; Cameron et al., 1968; Yerpude et al., 2016; Kore et al., 2014). The advantages of these types of detectors are the detector volume reduction, high-resolution measurements, and higher signal due to the higher ionization density (Karger et al., 2010). Dosimetric materials must satisfy certain important characteristics to be considered as a suitable TL dosimeter. Among the main requirements imposed on these materials are, to have a linearity response with the irradiation dose, high sensitivity for different radiation types, no dose rate dependence, a low energy dependence, low fading, and low Z effective to approximate that of human tissue (7.35–7.65) (Cameron et al., 1968). In general, luminescence dosimetry refers to the emission of photons from the dosimeter previously irradiated by different excitation methods, such as thermoluminescence (TL), optically stimulated luminescence (OSL), radiophotoluminescence (RPL), radioluminescence (RL) and scintillation. This review will focus on the passive use of

* Corresponding author. Institute of Physics, University of São Paulo, Rua do Matão, Travessa R, 187, CEP 05508-090, São Paulo, SP, Brazil.
E-mail addresses: clorenzo@if.usp.br (C.D. Gonzales-Lorenzo), ldfnasci@sckcen.be (L.F. Nascimento), kodaira.satoshi@qst.go.jp (S. Kodaira), monisebrito@usp.br (M.B. Gomes), watanabe@if.usp.br (S. Watanabe).

https://doi.org/10.1016/j.radphyschem.2020.109132
Received 27 April 2020; Received in revised form 1 July 2020; Accepted 29 July 2020
Available online 31 July 2020
0969-806X/

thermoluminescence dosimeters (TLD). Although some studies are describing the effect of the accelerated ion beam on phosphor material as TL dosimeters, literature is still very limited. Among luminescent detectors used in particle beam dosimetry, there is the $LiCaAlF_6$:Ce phosphor studied by Yerpude et al. (2016). This material was exposed to gamma radiation and carbon ion beam and their TL responses were compared displaying a change in the relative intensity/trapping parameters of the TL glow peaks. Kore et al. (2014) have produced by acid distillation method the Dy^{3+}-doped $CaMg_3(SO_4)_4$. This material doped with 0.2 mol% of Dy^{3+} was found to be 3.5 times more sensitive than a standard $CaSO_4$:Dy^{3+} phosphor with a stable dosimetric TL peak for C^{5+} ion irradiation. Nascimento et al. (2015) have studied the capability of RL dosimeter based on carbon-doped aluminum oxide (Al_2O_3:C) for absorbed dose-rate measurements during carbon radiotherapy. In recent years, there has been an increasing amount of literature about dosimeter materials based in silicate minerals either natural or synthetic compounds, such as beryl, tourmaline, quartz, jadeite, colourless topaz and natural wollastonite ($CaSiO_3$) (Watanabe et al., 2015; Souza et al., 2002, 2007a; 2007b; Gonzales-Lorenzo et al., 2018, 2020a; 2020b; Portakal et al., 2020). These materials have shown a high sensitivity to X-ray and gamma radiation. Concerning TL properties, these minerals show a dosimetric TL peak, low fading, and good reproducibility (Gonzales-Lorenzo et al., 2018, 2020b; Souza et al., 2002, 2007a, 2007b).

Gonzales-Lorenzo et al. (2020a, 2020b) have produced synthetic polycrystals of β-$CaSiO_3$ (pseudowollastonite) and their TL properties reported. This material shows O^- ion and F^+ defect centers in the lattice structure which behave like recombination centers in the TL process. These centers are responsible for the high-temperature TL peaks in β-$CaSiO_3$ (Gonzales-Lorenzo et al., 2020b). The high-temperature TL peak at about 250 °C shows good stability and a dosimetric behavior when irradiated at low gamma radiation dose, of the order of mGy to Gy, and when irradiated with high neutron fluence, of the order of 10^{13}-10^{16} n/cm^2. Besides in this material the high-temperature TL peaks display a low fading of about 7% in the first 48 h, after that time, there is no decay. This behavior makes the study of the $CaSiO_3$ of great interest, since higher temperature peaks are normally more stable at room temperature than lower temperature ones, and because it is possible the monitoring of the deposited gamma radiation through the intensity of the dosimetric and stable TL peak. On account of that, in this work pellets of calcium silicate were produced as gamma and ion beam dosimeters in an attempt to obtain useful data regarding the TL response of gamma, proton, and carbon ion beam-irradiated sensitive phosphors. Moreover, a study of the dose rate and energy dependence of the $CaSiO_3$ pellets by thermoluminescence response was performed.

2. Materials and methods

2.1. Synthesis

For the production of calcium silicate polycrystalline, $CaSiO_3$, the devitrification method was used (Magallanes-Perdomo et al., 2009). The synthesis process starts with weighing quantities of reagent grade CaO (Anidrol-PA ACS, 99.9%) and SiO_2. In this work, we used 12.0 g (44.4 wt%) CaO and 15.0 g (55.6 wt%) of SiO_2 (Kotsis and Balogh, 1989). These reagents then placed in an oven heated to 1500 °C to melt the above mixture, for 2 h. The melt is then cooled slowly using a temperature controller so that the room temperature is reached after about 24 h. After these procedures, a polycrystalline material is obtained.

This polycrystalline sample of $CaSiO_3$ was crushed and sieved to retain grains smaller than 80 μm in diameter. XRD data of this powder sample at room temperature were obtained on Rigaku Miniflex 300 diffractometer with Cu $K_{\alpha 1}$ (0.15406 nm) radiation between 10 and 60 at a 0.02° (in 2θ) scanning step and a 1 s step time.

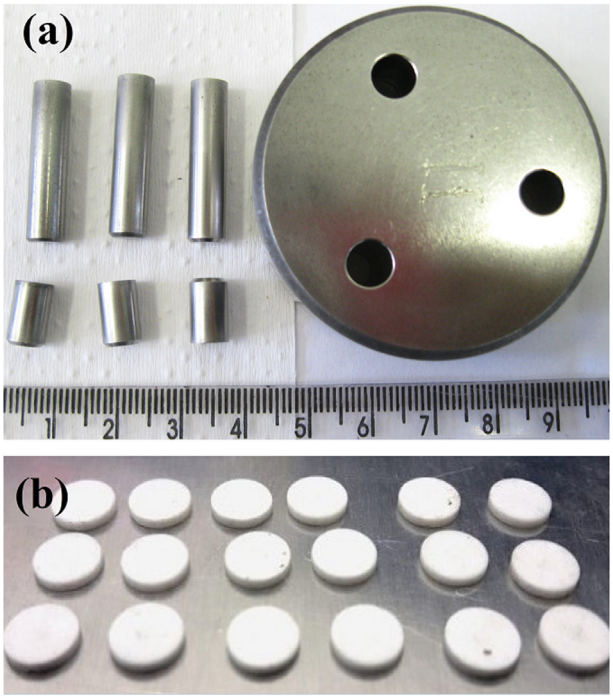

Fig. 1. (a) Steel device and steel pins for pellets production, and (b) pellets of $CaSiO_3$ of 6 mm in diameter and 1 mm thick.

2.2. Production of calcium silicate pellets

To improve the handling and the mass standardization of $CaSiO_3$ samples, powder of this polycrystal will be used to pellet production. The procedure for pellet production is given by the following stages: (a) *Milling process*: polycrystalline sample of $CaSiO_3$ was crushed and sieved to retain grains smaller than 80 μm in diameter. This powder is placed in a sealed container together with two milling alumina spheres. Then, the container is left in a mill for 24 h to homogenize and reduce the particle size of the sample (smaller than 80 μm). (b) *Powder compaction*: at this stage, a steel device with three 6 mm diameter channels was used as can be seen from Fig. 1(a). Later, 50 mg of the powder, obtained in the previous stage, is placed inside the hole. Previously, steel pins are also placed on the bottom and on top of the powder to keep it fixed inside the steel device. The device with samples inside is carried to the press and subjected to a pressure of 11 ton/cm^2 using a hydraulic press. Later, pellets of 6 mm in diameter and 1 mm thick but not resistant enough to handling are obtained. (c) *Thermal sintering*: using the thermal sintering technique the pellets obtained previously is carried at about 1200 °C for 30 min (best condition of time and temperature to obtain suitable hardness pellets) and then cooled slowly until it reaches room temperature. After that, a handling-resistant pellet is obtained as shown in Fig. 1(b). Preparation and sintering of the powder were performed at the Ionic Crystals, Thin Films and Dating Laboratory (LACIFID, for its acronym in Portuguese) of the University of São Paulo, whilst the pellets compression was carried out at the Radiations Metrology Department of the Nuclear and Energy Research Institute (IPEN, for its acronym in Portuguese).

2.3. Photon irradiation

Pellets of $CaSiO_3$ were irradiated with different X-ray energies at the Dosimetry Laboratory of the University of São Paulo to know the energy dependence of this material. For this purpose, the irradiation with 22, 40, 80, and 150 keV effective energies from an X-ray tube Philips MG 450 were carried out. Furthermore, to know the dose-response behavior and dose rate dependence, pellets of $CaSiO_3$ were also irradiated with

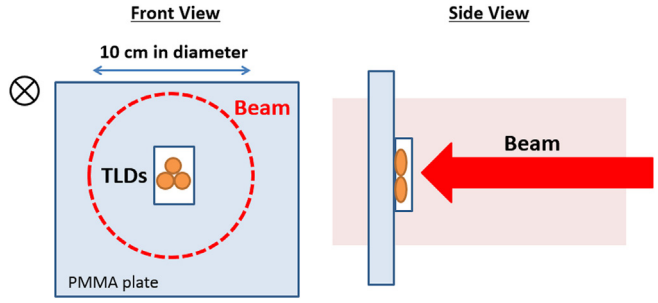

Fig. 2. Irradiation design of calcium silicate pellets with proton and carbon ion beam at NIRS.

gamma radiation from ^{137}Cs and ^{60}Co sources from IPEN. A panoramic type ^{137}Cs source of gamma rays with a dose rate of 33.03 mGy/h at 30 cm from the source and a panoramic type ^{60}Co source with a dose rate of 7.88 Gy/h at 40 cm from the source. The gamma irradiation was performed at room temperature and under conditions of electronic equilibrium using a PMMA plate of 3 mm thick acrylic layers placed on each side of the $CaSiO_3$ pellet, covering it completely.

2.4. Particle beam irradiation

Pellets of $CaSiO_3$ produced previously were irradiated with proton and carbon ion beams from an upper synchrotron of Heavy Ion Medical Accelerator (HIMAC) at the National Institute of Radiological Sciences (NIRS) in Chiba, Japan. The beam intensity was monitored and controlled with a beam monitor (parallel plate ionization chamber) installed in front of samples (Kanai et al., 1999). The monitor count is characterized by the absorbed dose at the sample measured with a Markus ionization chamber (Kanai et al., 2004).

The experimental procedure is given by the following stages: (a) first, 3 pellets in a plastic bag were attached in the irradiation position, that is, on the center of the PMMA plate as shown in Fig. 2. (b) Pellets were irradiated at 160 MeV proton beam and 290 MeV/n carbon ion beam. The beam has spread over a uniform area of 10 cm (with an uncertainty of about 5%) in diameter at the irradiation position as can been seen from Fig. 2. (c) The given dose was monitored with an ionization chamber installed in the beam line. Doses at which pellets were exposed varies from 1 mGy to 10 Gy.

2.5. TL measurements

Harshaw TL reader model 4500 in a nitrogen atmosphere was used for the TL measurements; the heating rate was kept at 4 °C/s. Luminescence in this equipment was detected by a Hamamatsu R647 photomultiplier tube through a Schott KG1 filter (transmission band 330–690 nm). Five TL reading measurements were carried out to obtain an average TL glow curve. All TL readings were carried out at least 48 h after the irradiation took place, time enough to reach the stability of the TL peaks in $CaSiO_3$ polycrystals.

3. Results and discussion

3.1. X-ray diffraction studies

The diffractogram of the $CaSiO_3$ synthetic material is shown in Fig. 3. All the diffraction peaks in the spectrum are coincident of the pseudowollastonite (β-$CaSiO_3$) crystal pattern and of the cristobalite-low (polymorphic of quartz - SiO_2). Both phases are identified with 01-074-0874 and 01-071-0785 PDF-2 files of the X'Pert HighScore Plus software (Speakman, 2012) for pseudowollastonite and cristobalite-low, respectively. This software was used for the refinement and to determine the percentage of each crystalline phase in the sample. The

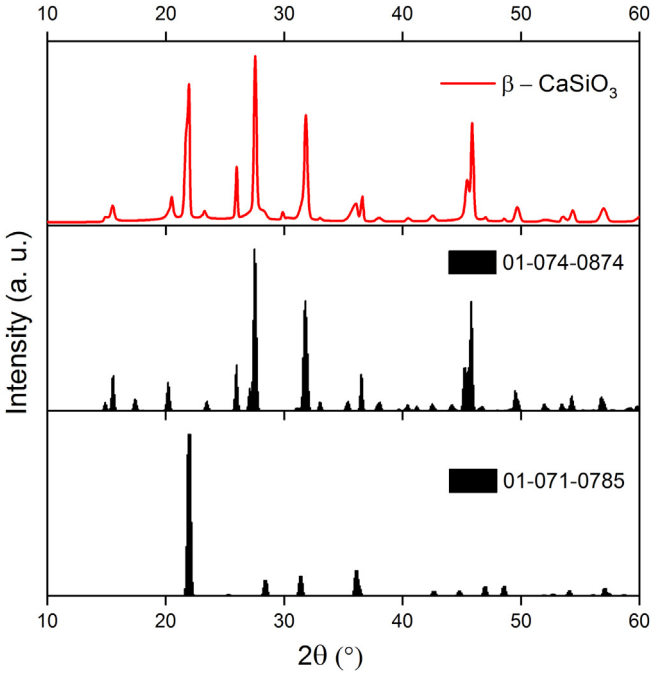

Fig. 3. XRD pattern of $CaSiO_3$ produced in this work, compared with XRD patterns from PDF-2 files: 01-074-0874 (pseudowollastonite) and 01-071-0785 (cristobalite low) - X'Pert HighScore program (Speakman, 2012).

results have shown that 96% of the sample is belonging to pseudowollastonite and 4% to cristobalite-low. In this way, the β-$CaSiO_3$ type polycrystalline structure dominates this sample.

3.2. Thermoluminescence studies

TL glow curves of $CaSiO_3$ pellets irradiated with gamma dose from 1 mGy to 100 mGy using a ^{137}Cs source are shown in Fig. 4(a). These curves show one prominent well-defined peak at about 169 °C, and two possible peaks at about 270 and 320 °C.

The prominent peak at about 169 °C shown in Fig. 4(a) is unstable at room temperature, that is, this peak could show a high fading (McKeever, 1985). According to McKeever (1985), a TL peak above 200 °C is recommended for dosimetry purposes. For that reason, previous thermal annealing of 215 °C for 10 s was carried out before the TL measurement to fade the TL peak at 169 °C. Fig. 4(b) shows these TL glow curves of $CaSiO_3$ pellets irradiated with gamma dose from 1 mGy to 100 mGy (^{137}Cs source) after the previous thermal annealing mentioned above. Therefore, it is possible to observe in Fig. 4(b) the two high-temperature peaks at about 270 and 320 °C.

Fig. 5 shows the maximum TL response of the peak at about 270 °C of $CaSiO_3$ in pellets as a function of gamma irradiation dose, for doses ranging from 1 mGy to 5 Gy using ^{137}Cs (from 1 to 100 mGy) and ^{60}Co (from 0.5 to 5 Gy) sources. An appropriate correction has been done due to small differences in TL intensities using both sources with different dose rates (see Fig. 7). Each point is the average of five pellets measured. Analyzing the dose-response curves with log axes in the same scale, as shown in Fig. 5. It is observed that the TL response of peak at 270 °C has a linear behavior from 1 mGy to 5 Gy, with a calibration equation, equals to $I_{TL} = 0.375 \cdot Dose$. As a result, the minimum detectable dose (MDD) was also calculated. The MDD value is obtained intercepting the linear fit behavior of TL peak with three times the standard deviation of zero dose TL reading ($3\sigma_{TL}$) (Gugliotti et al., 2018). Accordingly, an MDD of about 75 μGy was obtained as can be observed from Fig. 5. It is important to be mention that fading studies of all TL peaks of this polycrystalline $CaSiO_3$ have been reported in previous work (Gonzales-Lorenzo et al., 2020b).

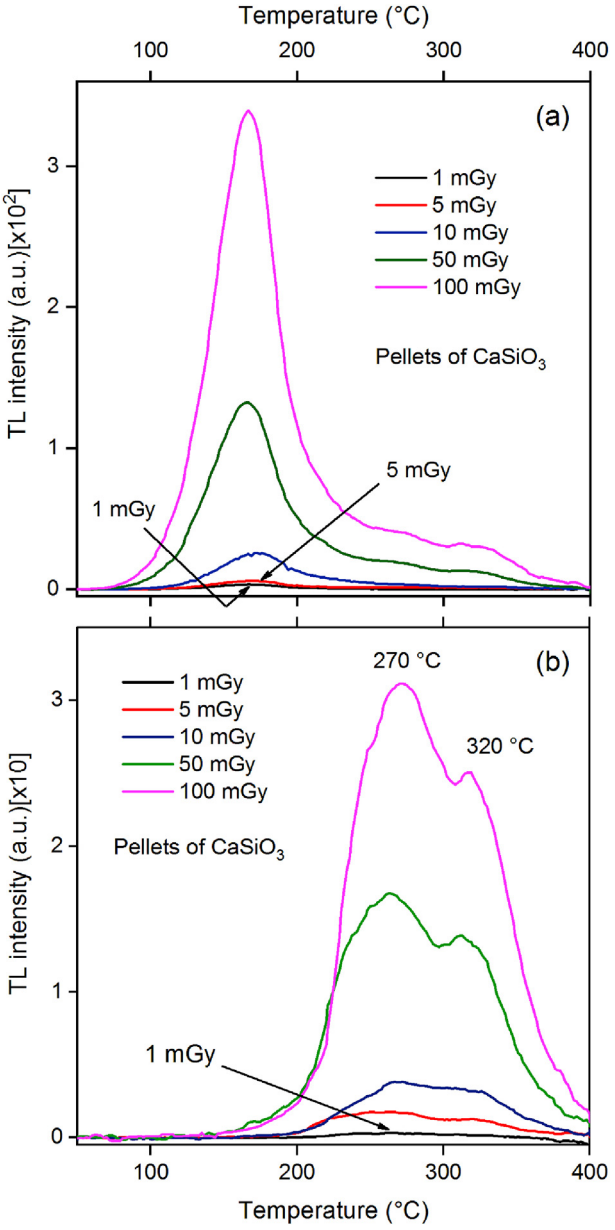

Fig. 4. (a) TL glow curves of pellets of $CaSiO_3$ irradiated with gamma dose from 1 mGy to 100 mGy using a ^{137}Cs source, and (b) glow curves after previous thermal annealing of about 215 °C for 10 s. A heating rate of 4 °C/s was used in each measurement.

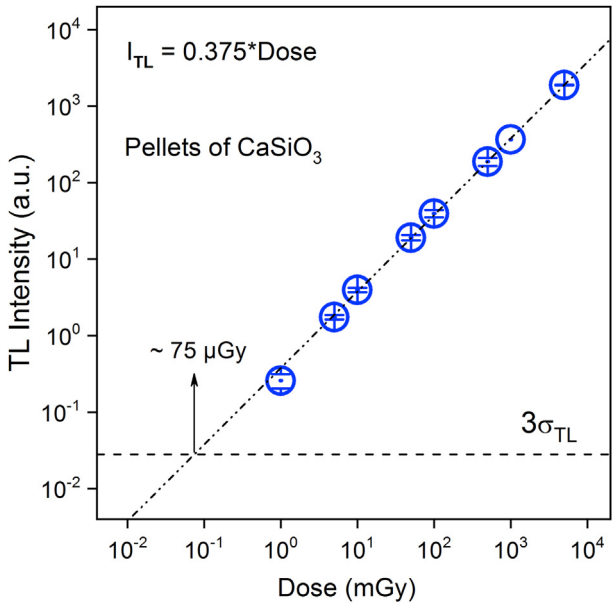

Fig. 5. TL intensity behavior of the 270 °C peak as a function of gamma radiation doses from 1 to 100 mGy (^{137}Cs) and from 0.5 to 5 Gy (^{60}Co), and the minimum detectable dose of synthetic $CaSiO_3$ pellets.

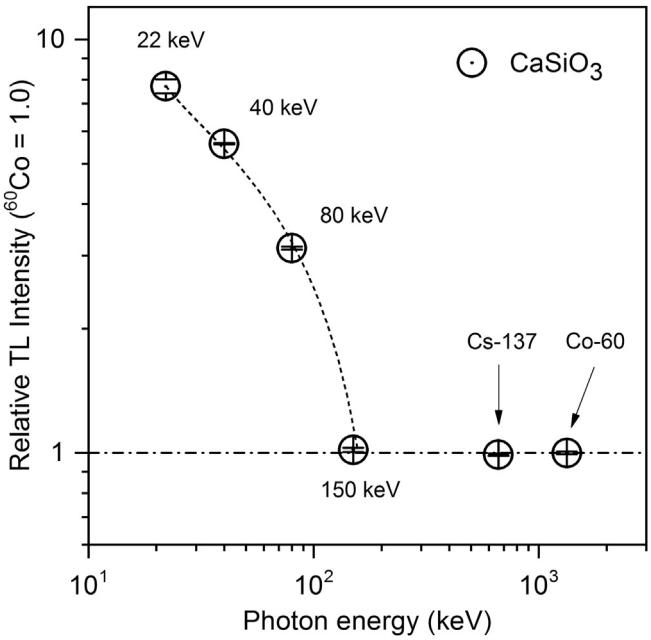

Fig. 6. Relative TL intensity response as a function of photon energy for pellets of $CaSiO_3$. TL response is normalized to the response of ^{60}Co gamma radiation.

3.3. Energy dependence of $CaSiO_3$ pellets

The relative TL intensity (TL peak at 270 °C) normalized to that TL response with ^{60}Co gamma radiation as a function of the photon energy is shown in Fig. 6. In all cases, the proton dose was estimated to be about 10 mGy to avoid supralinearity effects. It can be observed that between 22 and 150 keV effective energy the relative TL intensity decreases until reaching the value of 1, after that, this intensity seems to remain constant with the increase in energy as can be seen from Fig. 6.

This behavior is due to the different interaction of photons with the sample. Three main types of these interactions are known to be important in imparting energy to the sample during irradiation according to the photon energy. These are the Compton and photoelectric effect, and pair production. For low Z-effective materials such as carbon, water, or human tissue the region of Compton-effect dominance is very broad, from about 20 keV to 30 MeV (Attix, 2004). For $CaSiO_3$ pellets, between 20 and 150 keV, photoelectric interactions are possibly dominant, after that the Compton interaction will be prevalent.

Additionally, the concept de effective atomic number Z_{eff} has been introduced to characterize the energy response of different materials. Eq. (1) shows the calculation of the effective atomic number, where a_i is the fractional electron content of element i with atomic number Zi. The value of m varies from 3 to 4 with a reasonable value of m = 3.5 (Kase et al., 1987; Bos, 2001). In this manner, the effective atomic number of the $CaSiO_3$ using a value of m = 3.5 is about Z_{eff} = 15.72. This result is similar to the effective atomic number for $CaSO_4$, Z_{eff} = 15.62 (Bos, 2001). The high Z_{eff} found for $CaSiO_3$ contributes to more energy being deposited in this material due to a higher probability for photoelectric effect and higher mass-energy absorption coefficient compared to a

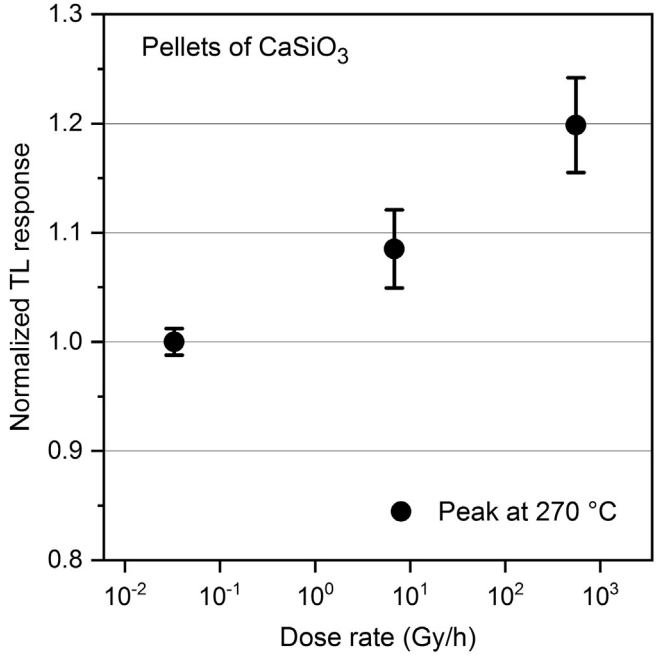

Fig. 7. Dose rate dependence response of synthetic $CaSiO_3$ pellets using a ^{137}Cs source. The response is normalized to the reading at a dose rate of 33.03 mGy/h. Three detectors were used at each dose rate setting.

tissue-equivalent material. The luminescent response for high Z_{eff} materials usually needs to be corrected due to the high dependence on beam energy. This can be performed using either two materials of different Z_{eff} or using special filters that absorb low energy photons, thus modifying the energy response of the material used (Yukihara and McKeever, 2011).

$$Z_{eff} = \sqrt[m]{\sum_i a_i Z_i^m} \quad (1)$$

3.4. Dose rate dependence studies

In this subsection, a dose rate dependence study of $CaSiO_3$ pellets was carried out. From Fig. 7 we can see the normalized TL response (peak at 270 °C) as a function of the dose rate, normalized to the response at the dose rate of 33.03 mGy/h. Three rate doses of 33.03 mGy/h (from ^{137}Cs source), 6.82 Gy/h, and 555 Gy/h (the last two from different ^{60}Co sources) were used in this experiment. In conventional radiotherapy, photon or electron beam from a linear accelerator, dose rates used clinically 0.1–0.2 Gy/s are usual. However, recent studies where ultra-high dose rate irradiation is involving (more than 100 Gy/s); termed FLASH radiotherapy (FLASH-RT) has appeared as an innovative modality able to improve therapeutic responses and limiting normal tissue injury (Spitz et al., 2019). In this way, luminescence dosimeters that are not influenced or have a negligible influence by the dose rate in addition to having a low energy-beam dependence are required for use in FLASH-RT. In this case, between 33.03 mGy/h and 555 Gy/h dose rates, normalized TL intensity increase by about 16.6%, as can be observed in Fig. 7. As a consequence, a suitable correction should be performed when $CaSiO_3$ pellets are irradiated at different dose rates. However, a study of this effect for dose rates higher than 555 Gy/h (~1.54 Gy/s) is necessary, especially on the order of hundreds of Gy/s.

3.5. Proton and carbon ion irradiation studies

TL glow curves of $CaSiO_3$ pellets irradiated with proton beam with doses from 10 mGy to 1 Gy are shown in Fig. 8(a). Moreover, TL glow curves of $CaSiO_3$ pellets irradiated with a carbon beam with doses from 10 mGy to 1 Gy are shown in Fig. 8(b). Both emission curves show one well-defined peak at about 165–170 °C, a peak at about 270 °C which is overshadowed by the intensity of the low-temperature peak, and a high-temperature peak at 320 °C. These TL glow curves are similar to those of the gamma irradiation case as shown in Fig. 4.

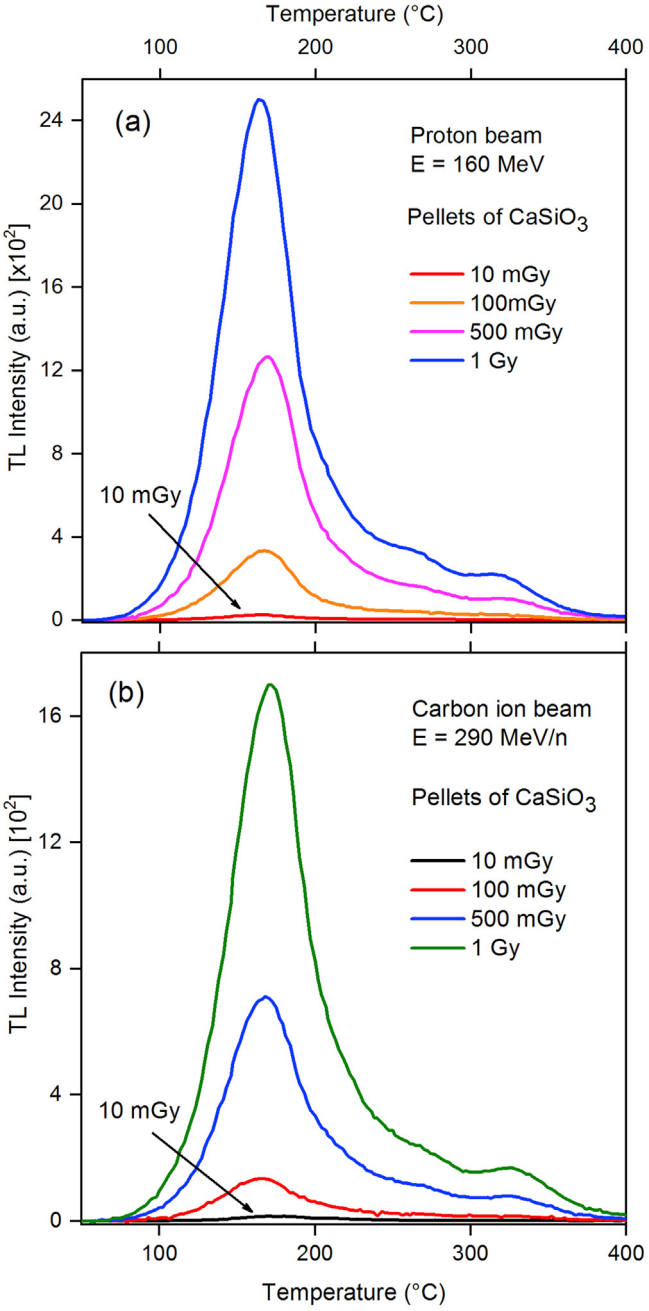

Fig. 8. TL glow curves of $CaSiO_3$ pellets (a) irradiated at 160 MeV proton beam with dose from 10 mGy to 1 Gy and (b) irradiated at 290 MeV/n carbon ion beam from 10 mGy to 1 Gy. A heating rate of 4 °C/s was used in each measurement.

Fig. 9(a) shows the maximum TL response of the peak at about 270 °C as a function of proton radiation dose from 5 mGy to 1 Gy found using an ion chamber. This result has been compared with the dose-response curve for the case of gamma irradiation from 1 mGy to 5 Gy (see Fig. 6). Analyzing the dose-response curves with log axes in the same scale in Fig. 9(a), it can be observed that TL response of peak at 270 °C has a linear behavior from 5 mGy to 1 Gy with a calibration

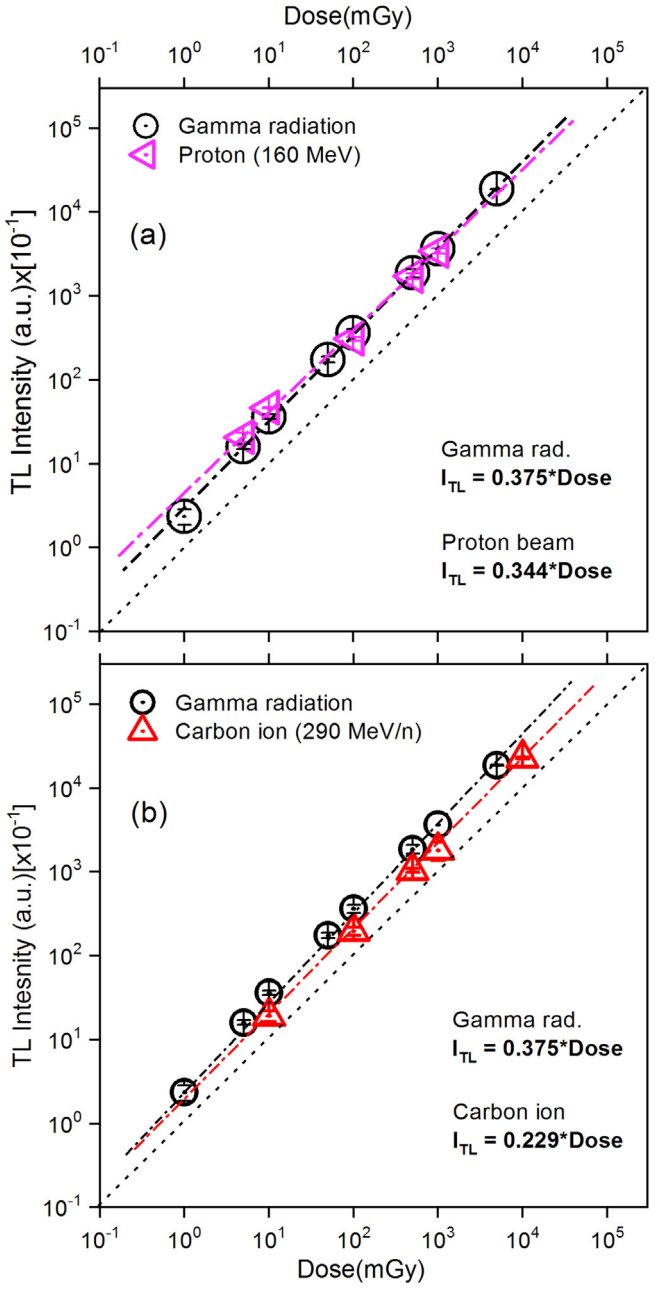

Fig. 9. Dose-response curve (a) for proton beam irradiation on $CaSiO_3$ pellets from 5 mGy to 1 Gy (pink triangles), and (b) for carbon beam irradiation from 10 mGy to 10 Gy (red triangles). Both curves are compared to that of the gamma radiation case (black circle). The dotted line indicates linearity. (For interpretation of the references to colour in this figure legend, the reader is referred to the Web version of this article.)

equation equals to I_{TL} = 0.344·Dose. The slope of the dose-response curve for proton irradiation is slightly less than the dose-response curve for gamma irradiation. Furthermore, Fig. 9(b) shows the maximum TL response of the peak at about 270 °C of $CaSiO_3$ in pellets as a function of carbon ion radiation dose from 10 mGy to 10 Gy found using an ion chamber. This result has been also compared with the dose-response curve for the case of gamma irradiation. Analyzing the dose-response curves with log axes in the same scale in Fig. 9(b), it can be observed that the TL response of peak at 270 °C peak has a linear behavior from 10 mGy to 10 Gy with a calibration equation equals to I_{TL} = 0.229·Dose. The slope of the dose-response curve for carbon irradiation is less than the dose-response curve for gamma irradiation.

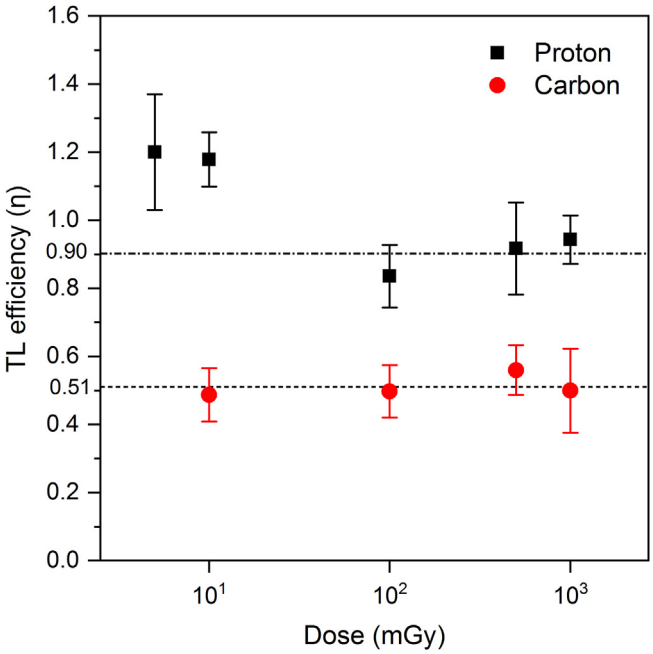

Fig. 10. Relative TL efficiency of $CaSiO_3$ detectors versus particle dose for proton and carbon beams. The data points represent the average of three TL detectors and the error bars are the experimental standard deviation of the data.

The differences in the slope shown in Fig. 9 are produced because the deposition dose during proton and carbon ion irradiation depends on the linear energy transference (LET) (Avila et al., 1999; Bilski et al., 1997; Geiß et al., 1998). An analytical study of accelerated particle interaction of proton and carbon ion beam on $CaSiO_3$ material will be the subject of future work.

Besides, when TLD detectors are exposed to other radiation types than gamma the relative TL efficiency term $\eta_{k\gamma}$ is usually used to know the ionization density dependence and supralinear effects on the material (Sądel et al., 2013; Bilski, 2006). Relative TL efficiency $\eta_{k\gamma}$ is defined as follows (Spurný, 2004; Bilski, 2011):

$$\eta_{k\gamma} = \frac{I_k/D_k}{I_\gamma/D_\gamma} \quad (2)$$

where I_k and I_γ are TL intensities after radiation k and after reference gamma radiation. D_k and D_γ are the corresponding values of absorbed dose. I_k/D_k is the efficiency associated with the radiation type k. Fig. 10 shows the relative efficiency of $CaSiO_3$ pellets as a function of the ion doses up to 1 Gy. As can be observed in this figure the relative efficiency for proton beam appears to exceed unity (i.e. the efficiency is higher than that for gamma-rays) from 5 to 10 mGy dose range. However, from 100 mGy to 1 Gy the proton efficiency is inferior to unity (i.e. the efficiency is lower than that for gamma-rays) reaching a value of about 0.90. To understand this behavior or to be certain if this effect is real, further studies are necessary, such as repeated proton exposure with careful monitoring of gamma and ion dose calibration. On the other hand, for the carbon ion beam case, the relative efficiency seems to follow a unique value at around 0.51. Consequently, relative efficiencies displayed in Fig. 10, for proton (160 MeV) from 100 mGy to 1 Gy and for carbon ion beam (290 MeV/n) from 10 mGy to 1 Gy are independent of the particle dose in the mentioned range. The relative efficiency values of about 0.90 for proton and 0.51 for carbon ion depend on the ionizing density (Sądel et al., 2013). That is, for a weakly ionizing radiation type (energy of few hundreds of keV), the relative efficiency is roughly constant (with a value equal to or close to unity) as a function of the LET. For a strongly ionizing radiation type, the relative efficiency usually decreases with increasing LET, up to values below 0.4 for LET values of the order of several hundreds of keV/μm (Bilski, 2006;

Sawakuchi et al., 2010).

4. Conclusions

Pellets of $CaSiO_3$ after gamma, proton, and carbon beam irradiation display the same shape of the TL glow curve with a prominent peak at about 169 °C. After the previous annealing of 215 °C during 10 s of irradiated $CaSiO_3$ pellets, TL glow curves of this material show two high-temperature and stable peaks at about 270 and 320 °C. Dose-response curve of $CaSiO_3$ pellets after gamma irradiation shows a linear behavior from 1 mGy to 5 Gy with a calibration equation: I_{TL} = 0.375·Dose. As a result, MDD for the $CaSiO_3$ detector was found to be 75 μGy.

From the energy dependence of the $CaSiO_3$ pellets we can observe that between 22 and 150 keV the relative TL intensity decrease, after that, it seems to remain constant with increasing photon energy. This is possibly due to the high dominant photoelectric effect between 22 and 150 keV followed by a prevailing Compton effect for energies greater than 150 keV.

The calculated effective atomic number found for $CaSiO_3$ was Z_{eff} = 15.72. Consequently, this material has a high energy beam dependence due to a higher probability for photoelectric effect and a higher mass-energy absorption coefficient compared to a tissue-equivalent material. On account of that, different methods to correct the energy response must be carried out.

Dose rate dependence of $CaSiO_3$ pellets has shown that, between 33.03 mGy/h and 555 Gy/h dose rates, normalized TL intensity increase by about 16.6%. Accordingly, a suitable correction must be performed when $CaSiO_3$ pellets are irradiated at different dose rates. Supplementary study of the TL dependence for a higher dose rate than 555 Gy/h (~1.54 Gy/s) will be the subject of future works.

For proton irradiation, the dose-response curve has a linear behavior from 5 mGy to 1 Gy with a calibration equation equals to I_{TL} = 0.344·Dose. Moreover, for ion carbon irradiation the dose-response curve has a linear behavior from 10 mGy to 10 Gy with a calibration equation equals to I_{TL} = 0.229·Dose. The slope of the dose-response curve for particle irradiation is slightly less than that of the dose-response curve for gamma irradiation due to the deposition dose during proton and carbon ion irradiation depends on the linear energy transference (LET). An analytical study of accelerated particle interaction on $CaSiO_3$ pellets will be proposed as part of future work.

Relative efficiencies of $CaSiO_3$ pellets for protons (160 MeV) and carbon ion (290 MeV/n) are independent of the particle dose in the range from 100 mGy to 1 Gy for proton and from 10 mGy to 1Gy for carbon ion, respectively. These constant relative efficiency values are about 0.90 for proton and 0.51 for carbon ion.

CRediT authorship contribution statement

Carlos D. Gonzales-Lorenzo: Conceptualization, Investigation, Writing - original draft. **Luana F. Nascimento:** Validation, Formal analysis, Visualization. **Satoshi Kodaira:** Supervision, Methodology, Investigation. **Monise B. Gomes:** Formal analysis, Writing - review & editing. **Shigueo Watanabe:** Supervision, Funding acquisition, Resources.

Declaration of competing interest

The authors declare that they have no known competing financial interests or personal relationships that could have appeared to influence the work reported in this paper.

Acknowledgments

This work was performed as a part of accelerator experiments of the Research Project (H386) at NIRS-HIMAC. The authors would like to express our thanks to Ms. E. Somessari and Mr. Aldo Oliveira from the Institute for Energy and Nuclear Researches (IPEN), Brazil, for kindly carrying out the gamma irradiation of the samples. To Dr. Nancy Kuniko Umisedo from the Dosimetry Laboratory at the University of São Paulo, Brazil, for kindly carrying out the X-rays irradiation of the samples. To HIMAC team for their kind support throughout the experiments. This work was carried out with partial financial support from Fundação de Amparo à Pesquisa do Estado de São Paulo - FAPESP, Brazil (Process number 2014/03085-0). To Consejo Nacional de Desarrollo Científico y Tecnológico - CNPq, Brazil, for fellowship to C.D. Gonzales-Lorenzo (Process number 162741/2015-4).

Appendix A. Supplementary data

Supplementary data to this article can be found online at https://doi.org/10.1016/j.radphyschem.2020.109132.

References

Akselrod, M.S., Kortov, V.S., Kravetsky, D.J., Gotlib, V.I., 1990. Highly sensitive thermoluminescent anion-defective alpha-Al_2O_3:C single crystal detectors. Radiat. Protect. Dosim. 32, 15–20. https://doi.org/10.1093/oxfordjournals.rpd.a080715.

Attix, F.H., 2004. Introduction to Radiological Physics and Radiation Dosimetry. WILEY-VCH Verlag GmbH & Co.

Avila, O., Gamboa-deBuen, I., Brandan, M.E., 1999. Study of the energy deposition in LiF by heavy charged particle irradiation and its relation to the thermoluminescent efficiency of the material. J. Phys. D Appl. Phys. 32, 1175–1181. https://doi.org/10.1088/0022-3727/32/10/315.

Barth, W., Dahl, L., Glatz, J., Groening, L., Richter, S., Yaramishev, S., 2003. Application of beam diagnostics for intense heavy ion beams at the GSI UNILAC. Proc. DIPAC 161–163.

Bilski, P., Budzanowski, M., Hoffmann, W., Molokanov, A., Olko, P., Waligorski, M.P.R., 1997. Investigation of efficiency of thermoluminescence detectors for particle therapy beams. Radiat. Protect. Dosim. 70, 501–504. https://doi.org/10.1093/oxfordjournals.rpd.a032006.

Bilski, P., 2006. Response of various LiF thermoluminescent detectors to high energy ions – results of the ICCHIBAN experiment. Nucl. Instrum. Methods B. 251, 121–126. https://doi.org/10.1016/j.nimb.2006.05.012.

Bilski, P., 2011. Calculation of the relative efficiency of thermoluminescent detectors to space radiation. Radiat. Meas. 46, 1728–1731. https://doi.org/10.1016/j.radmeas.2011.04.002.

Bos, A.J.J., 2001. High sensitivity thermoluminescence dosimetry. Nucl. Instrum. Methods B. 184, 3–28. https://doi.org/10.1016/S0168-583X(01)00717-0.

Cameron, J.R., Suntharalingam, N., Kenney, G.N., 1968. Thermoluminescent Dosimetry. The University of Wisconsin Press, Madison, USA.

Fujisawa, H., Genik, P.C., Kitamura, H., Fujimori, A., Uesaka, M., Kato, T.A., 2013. Comparison of human chordoma cell-kill for 290 MeV/n carbon ions versus 70 MeV protons in vitro. Radiat. Oncol. 8, 91. https://doi.org/10.1186/1748-717X-8-91.

Geiß, O.B., Krämer, M., Kraft, G., 1998. Efficiency of thermoluminescent detectors to heavy charged particles. Nucl. Instrum. Methods B. 142, 592–598. https://doi.org/10.1016/S0168-583X(98)00325-5.

Gonzales-Lorenzo, C.D., Watanabe, S., Cano, N.F., Ayala-Arenas, J.S., Bueno, C.C., 2018. Synthetic polycrystals of $CaSiO_3$ un-doped and Cd, B, Dy, Eu-doped for gamma and neutron detection. J. Lumin. 201, 5–10. https://doi.org/10.1016/j.jlumin.2018.04.037.

Gonzales-Lorenzo, C.D., Watanabe, S., Cavalieri, T.A., Cano, N.F., Gundu Rao, T.K., Chubaci, J.F.D., Carmo, L.S., Bueno, C.C., 2020a. Calculated and experimental response of calcium silicate polycrystalline to high and very-high neutron doses. Radiat. Phys. Chem. 172, 108820. https://doi.org/10.1016/j.radphyschem.2020.108820.

Gonzales-Lorenzo, C.D., Gundu Rao, T.K., Cano, N.F., Silva-Carrera, B.N., Rocca, R.R., Cuevas-Arizaca, E.E., Ayala-Arenas, J.S., Watanabe, S., 2020b. Thermoluminescence and defect centers in β-$CaSiO_3$ polycrystal. J. Lumin. 217, 116783. https://doi.org/10.1016/j.jlumin.2019.116783.

Gugliotti, C., Moriya, K., Tatumi, S., Mittani, J., 2018. Synthesis and luminescence studies of Tb-doped MgO-$MgAl_2O_4$-Mg_2SiO_4 ceramic for use in radiation dosimetry. Appl. Radiat. Isot. 135, 219–223. https://doi.org/10.1016/j.apradiso.2018.01.040.

Haberer, T., 2002. Advances in charged particle therapy. AIP Conf. Proc. 610, 157–166. https://doi.org/10.3390/cancers10030066.

Jaffray, D.A., Carlone, M., Menard, C., Breen, S., 2010. Image-guided radiation therapy: emergence of MR-guided radiation treatment (MRgRT) systems. In: Medical Imaging 2010: Physics of Medical Imaging. vol. 7622. pp. 29–40. https://doi.org/10.1117/12.848608.

Kanai, T., Endo, M., Minohara, S., Miyahara, N., Koyama-ito, H., Tomura, H., Matsufuji, N., Futami, Y., Fukumura, A., Hiraoka, T., Furusawa, Y., Ando, K., Suzuki, M., Soga, F., Kawachi, K., 1999. Biophysical characteristics of HIMAC clinical irradiation system for heavy-ion radiation therapy. Int. J. Radiat. Oncol. Biol. Phys. 44, 201–210. https://doi.org/10.1016/S0360-3016(98)00544-6.

Kanai, T., Fukumura, A., Kusano, Y., Shimbo, M., Nishio, T., 2004. Cross-calibration of

ionization chambers in proton and carbon beams. Phys. Med. Biol. 49, 771–781. https://doi.org/10.1088/0031-9155/49/5/008.
Karger, C.P., Jäkel, O., Palmans, H., Kanai, T., 2010. Dosimetry for ion beam radiotherapy. Phys. Med. Biol. 55, 193–234. https://doi.org/10.1088/0031-9155/55/21/r01.
Kase, K.R., Bjarngard, B.E., Attix, F.H., 1987. The Dosimetry of Ionizing Radiation, first ed. Elsevier Science.
Kore, B.P., Dhoble, N.S., Lochab, S.P., Dhoble, S.J., 2014. A new highly sensitive phosphor for carbon ion dosimetry. RSC Adv. 4, 49979–49986. https://doi.org/10.1039/C4RA08742A.
Kotsis, I., Balogh, A., 1989. Synthesis of wollastonite. Ceram. Int. 15, 79–85. https://doi.org/10.1016/0272-8842(89)90018-7.
Kry, S.F., Alvarez, P., Cygler, J.E., DeWerd, L.A., Howell, R.M., Meeks, S., O'Daniel, J., Reft, C., Sawakuchi, G., Yukihara, E.G., Mihailidis, D., 2020. AAPM TG 191: clinical use of luminescent dosimeters: TLDs and OSLDs. Med. Phys. 47, 19–51. https://doi.org/10.1002/mp.13839.
Lakshmanan, A., 2001. A new high sensitive $CaSO_4$:Dy thermostimulated luminescence phosphor. Phys. Status Solidi A 186, 153–166. https://doi.org/10.1002/1521-396X(200107)186:1<153::AID-PSSA153>3.0.CO;2-W.
Magallanes-Perdomo, M., Pena, P., De Aza, P.N., Carrodeguas, R.G., Rodríguez, M.A., Turrillas, X., De Aza, S., De Aza, A.H., 2009. Devitrification studies of wollastonite-tricalcium phosphate eutectic glass. Acta Biomater. 5, 3057–3066. https://doi.org/10.1016/j.actbio.2009.04.026.
McKeever, S.W.S., 1985. Thermoluminescence of Solids. Cambridge Uni. Press., Cambridge.
Mein, S., Rankine, L., Miles, D., Juang, T., Cai, B., Curcuru, A., Mutic, S., Fenoli, J., Adamovics, J., Oldham, Li and M., 2017. How feasible is remote 3D dosimetry for MR guided Radiation Therapy (MRgRT)? J. Phys. Conf. Ser. 847, 1–5. https://doi.org/10.1088/1742-6596/847/1/012056.
Mohamad, E.O., Makishima, H., Kamada, T., 2018. Evolution of carbon ion radiotherapy at the national Institute of radiological Sciences in Japan. Cancers 10, 1–22. https://doi.org/10.3390/cancers10030066.
Nakajima, T., Murayama, Y., Matsuzawa, T., Koyano, A., 1978. Development of a new highly sensitive LiF thermoluminescence dosimeter and its applications. Nucl. Instrum. Methods 157, 155–162. https://doi.org/10.1016/0029-554X(78)90601-8.
Nascimento, L.F., Vanhavere, F., Kodaira, S., Kitamura, H., Verellen, D., De Deene, Y., 2015. Application of Al_2O_3:C+ fibre dosimeters for 290 MeV/n carbon therapeutic beam dosimetry. Radiat. Phys. Chem. 115, 75–80. https://doi.org/10.1016/j.radphyschem.2015.06.001.
Obryk, B., Glaser, M., Mandi, I., Bilski, P., Olko, P., Sas-Bieniarz, A., 2011. Response of various types of lithium fluoride MCP detectors to high and ultra-high thermal neutron doses. Radiat. Meas. 46, 1882–1885. https://doi.org/10.1016/j.radmeas.2011.06.050.
Portakal, U., Kaynar, Ü.H., Dogan, T., Souadi, G.O., Ayvacikli, M., Canimoglu, A., Topaksu, M., Can, N., 2020. Thermoluminescence behaviour of europium doped magnesium silicate after beta exposure. Opt. Mater. 104, 109852. https://doi.org/10.1016/j.optmat.2020.109852.
Sądel, M., Bilski, P., Swakoń, J., Ptaszkiewicz, M., Boberek, M., Olko, P., 2013. Relative thermoluminescent efficiency of LiF detectors for proton radiation: batch variability and energy dependence. Radiat. Meas. 56, 205–208. https://doi.org/10.1016/j.radmeas.2013.01.052.
Sawakuchi, G.O., Sahoo, N., Gasparian, P.B.R., Rodriguez, M.G., Archambault, L., Titt, U., Yukihara, E.G., 2010. Determination of average LET of therapeutic proton beams using Al_2O_3:C optically stimulated luminescence OSL detectors. Phys. Med. Biol. 55, 4963–4976. https://doi.org/10.1088/0031-9155/55/17/006.
Souza, D.N., Lima, J.F., Valerio, M.E.G., Caldas, L.V.E., 2002. Performance of pellets and composites of natural colourless topaz as radiation dosemeters. Radiat. Protect. Dosim. 100, 413–416. https://doi.org/10.1093/oxfordjournals.rpd.a005902.
Souza, D.N., Melo, A.P., Caldas, L.V.E., 2007a. TL and TSEE response of Wollastonite-Teflon composites in X-ray beams. Nucl. Instrum. Methods A. 580, 338–341. https://doi.org/10.1016/j.nima.2007.05.170.
Souza, D.N., Melo, A.P., Oliveira, M.G., Caldas, L.V.E., 2007b. Dosimetric characterization of wollastonite-teflon composites. Phys. Status Solidi C 4, 1175–1178. https://doi.org/10.1002/pssc.200673869.
Speakman, S.A., 2012. Introduction to PANalytical X'Pert HighScore Plus v3.0. MIT Center for Materials Science and Engineering.
Spitz, D.R., Buettner, G.R., Petronek, M.S., St-Aubin, J.J., Flynn, R.T., Waldron, T.J., Limoli, C.L., 2019. An integrated physico-chemical approach for explaining the differential impact of FLASH versus conventional dose rate irradiation on cancer and normal tissue responses. Radiother. Oncol. 139, 23–27. https://doi.org/10.1016/j.radonc.2019.03.028.
Spurný, F., 2004. Response of thermoluminescent detectors to charged particles and to neutrons. Radiat. Meas. 38, 407–412. https://doi.org/10.1016/j.radmeas.2003.12.023.
Takada, E., 2010. Carbon ion radiotherapy at NIRS-HIMAC. Nucl. Phys. A 834, 730–735. https://doi.org/10.1016/j.nuclphysa.2010.01.132.
Tsujii, H., Mizoe, J., Kamada, T., Baba, M., Tsuji, H., Kato, H., Kato, S., Yamada, S., Yasuda, S., Ohno, T., Yanagi, T., Imai, R., Kagei, K., Kato, H., Hara, R., Hasegawa, A., Nakajima, M., Sugane, N., Tamaki, N., Takagi, R., Kandatsu, S., Yoshikawa, K., Kishimoto, R., Miyamoto, T., 2007. Clinical results of carbon ion radiotherapy at NIRS. J. Radiat. Res. 48, 1–13. https://doi.org/10.1269/jrr.48.A1.
Tsujii, H., 2014. History of charged particle radiotherapy. In: Tsujii, H., Kamada, T., Shirai, T., Noda, K., Tsuji, H., Karasawa, K. (Eds.), Carbon-Ion Radiotherapy. Springer, Tokyo.
Wambersie, A., Menzel, H.G., Andreo, P., DeLuca, P.M., Gahbauer, R., Hendry, J.H., Jones, D.T.L., 2011. Isoeffective dose: a concept for biological weighting of absorbed dose in proton and heavier-ion therapies. Radiat. Protect. Dosim. 143, 481–486. https://doi.org/10.1093/rpd/ncq410.
Watanabe, S., Cano, N.F., Carmo, L.S., Barbosa, R.F., Chubaci, J.F.D., 2015. High- and very-high-dose dosimetry using silicate minerals. Radiat. Meas. 72, 66–69. https://doi.org/10.1016/j.radmeas.2014.11.004.
Yerpude, M.M., Dhoble, N.S., Lochab, S.P., Dhoble, S.J., 2016. Comparison of thermoluminescence characteristics in γ-ray and C^{5+} ion beam-irradiated $LiCaAlF_6$:Ce phosphor. Luminescence 31, 1115–1124. https://doi.org/10.1002/bio.3080.
Yukihara, E.G., McKeever, S.W.S., 2011. Optically Stimulated Luminescence: Fundamentals and Applications. John Wiley & Sons.